# Extracellular Matrix Remodeling and Metalloproteinase Involvement during Intestine Regeneration in the Sea Cucumber *Holothuria glaberrima*

**José L. Quiñones, Rey Rosa, Dorcas L. Ruiz, and José E. García-Arrarás[1]**
*Department of Biology, University of Puerto Rico, Río Piedras, Puerto Rico 00931*

The sea cucumber, *Holothuria glaberrima*, has the capacity to regenerate its internal organs. Intestinal regeneration is accomplished by the thickening of the mesenteric border and the invasion of this thickening by mucosal epithelium from the esophagus and the cloaca. Extracellular matrix (ECM) remodeling has been associated with morphogenetic events during embryonic development and regeneration. We have used immunohistochemical techniques against ECM components to show that differential changes occur in the ECM during early regeneration. Labeling of fibrous collagenous components and muscle-related laminin disappear from the regenerating intestine and mesentery, while fibronectin labeling and 4G7 (an echinoderm ECM component) are continuously present. Western blots confirm a decrease in fibrous collagen content during the first 2 weeks of regeneration. We have also identified five 1,10-phenanthroline-sensitive bands in collagen gelatin zymographs. The gelatinolytic activities of these bands are enhanced during early stages of regeneration, suggesting that the metalloprotease activity is associated with ECM remodeling. Inhibition of MMPs *in vivo* with 1,10-phenanthroline, p-aminobenzoyl-Gly-Pro-D-Leu-D-Ala hydroxamate or N-CBZ-Pro-Leu-Gly hydroxamate produces a reversible inhibition of intestinal regeneration and ECM remodeling. Our results show that significant changes in ECM content occur during intestine regeneration in the sea cucumber and that the onset of these changes is correlated to the proteolytic activities of MMPs. © 2002 Elsevier Science (USA)

*Key Words:* echinoderm; extracellular matrix remodeling; ECM; epithelial tubular outgrowth; fibrosis; holothuroid; intestine regeneration; metalloproteases; metalloprotease inhibitors; morphogenesis; organogenesis; 1,10-phenanthroline; zymograph.

## INTRODUCTION

Extracellular matrix (ECM) molecules are known to participate in the regulation of organ development and in the differentiation of cells (Adams and Watt, 1993; Thesleff *et al.,* 1995; Ashkenas *et al.,* 1996). In animals, changes in ECM composition and regulated matrix degradation are common events during embryogenesis and tissue regeneration. ECM remodeling associated with organ morphogenesis and tissue regeneration has been reported in mammalian nephrogenesis (Tanney *et al.,* 1998; Wallner *et al.,* 1998), mice and rat mammary gland development (Talhouk *et al.,* 1991; Witty *et al.,* 1995; Uria and Werb, 1998; Schedin *et al.,* 2000), *Xenopus* organ development and

wound healing (Patterton *et al.,* 1995; Damjanovsky *et al.,* 1999, 2000; Carinato *et al.,* 2000), newt limb regeneration (Yang and Bryant, 1994; Miyazaki *et al.,* 1996; Nace and Tassava, 1995; Gassner and Tassava, 1997; Christensen and Tassava, 2000), rat liver regeneration (Kim *et al.,* 1997), gonadal formation in *Caenorhabditis elegans* (Belloch and Kimble, 1999), morphogenesis and head regeneration in *Hydra* (Yan *et al.,* 2000a,b; Leontovich *et al.,* 2000), and sea urchin embryogenesis (Wessel and McClay, 1987; Roe *et al.,* 1989; Ramachandran *et al.,* 1993; Quigley *et al.,* 1993; Vafa *et al.,* 1995, 1996; Robinson, 1997, Ingersoll and Wilt, 1998; Mayne and Robinson, 1996; Wardle *et al.,* 1999).

Skin wound healing provides one of the best documented examples of ECM remodeling involvement in the regeneration of tissues (Rooney and Kumar, 1993; Martin, 1997). During wound healing and regeneration of the vertebrate skin, the ECM is degraded (mostly collagen), and a tempo-

rary matrix is formed, consisting primarily of hyaluronic acid, fibronectin, and fibrin. This temporary matrix may incorporate instructive matrix molecules, such as other ECM molecules, and growth factors, which stimulate cell migration and proliferation. After restitution of tissues, the hyaluronic acid is degraded and a new collagen matrix is synthesized.

The matrix metalloproteases (MMPs) that degrade ECM components seem to be crucial to the onset of the matrix changes that occur during ECM remodeling. MMPs, including the collagenases, gelatinase/collagenase, and stromelysins, have been associated with morphoregulatory roles and shaping of organs during embryogenesis and regeneration (Matrisan, 1990, 1992; Massova *et al.,* 1998; Nagase and Woessner, 1999). These proteinases degrade at least one component of the ECM, they contain a zinc ion in their catalytic site and can be inhibited by chelating agents, tissue inhibitors of metalloproteinases (TIMPs), and synthetic peptides. During skin wound healing, at least three MMPs are up-regulated (Martin, 1997), and during amphibian limb regeneration, an increase in gelatinolytic activity in zymographs has been reported (Yang and Bryant, 1994; Miyazaki *et al.,* 1996). MMPs have also been detected in sea urchins, where they seem to play a significant role in development (Ghiglione *et al.,* 1994; Vafa and Nishioka, 1995; Lhomond *et al.,* 1996; Mayne and Robinson, 1996; Quigley *et al.,* 1993; Robinson, 1997; Ingersoll and Wilt, 1998). In gelatin zymographs, bands of gelatinolytic activities were detected in *Arbacia punctulata*, *Strongylocentrotus purpuratus*, and *Lytechinus pictus* during development, and these activities were found to increase during gastrulation (Quigley *et al.,* 1993; Vafa *et al.,* 1996).

Echinoderms exhibit a high capacity to regenerate their tissues and organs (Hyman, 1955). This capacity is best manifested in the members of the class Holothuroidea (Mosher, 1956; Bai, 1971; García-Arrarás *et al.,* 1998). When holothuroids are exposed to adverse stimuli, they respond by ejecting most of their internal organs. The ejected viscera are then regenerated. Our laboratory has developed the use of the sea cucumber *Holothuria glaberrima* as an excellent biological system for studying organogenesis in an adult organism. The intestinal system is the first to regenerate from a thickening that forms at the edges of the torn mesentery (García-Arrarás *et al.,* 1998). Here, we study the epithelial and connective tissue interaction, in particular the matrix remodeling, during intestine regeneration.

To determine whether changes in ECM composition occur during intestine regeneration, we have used immunohistochemical analysis for ECM molecules, such as collagen, fibronectin, laminin, and other interstitial fiber, and basal lamina components at different stages of regeneration. ECM molecular changes were analyzed, focusing on the collagen content and on the activities and possible involvement of MMPs. Our results provide important insights to the understanding of the role of ECM remodeling and tissue interactions during the regeneration of a complex organ.

## MATERIALS AND METHODS

### Animals

*Holothuria glaberrima* specimens were collected in the northeast coast of Puerto Rico and maintained in seawater aquaria at 22–24°C. Evisceration of animals was induced by KCl 0.35 M injections (2 ml) into the coelomic cavity. Prior to the dissections, animals were anesthetized with 6% $MgC1_2$ for 1 h.

### Immunohistochemistry

Tissues from noneviscerated (d-0), and regenerating animals at d-3, -7, -14, -21, -28, -42, and -65 after evisceration were fixed in picric–formaldehyde (Zamboni) fixative, washed in ethanol, DMSO, and 0.1 M PBS, pH 7.4, and kept in PBS/sucrose 30% until use (see García-Arrarás *et al.,* 1998). Tissues were mounted in embedding medium (OCT; Miles Inc., Elkahart, IN), sectioned (20 $\mu$m) in a cryostat microtome (Leica CM 1900) at −30°C, and sections were recovered on poly-lysine-treated glass slides. Unless stated otherwise, tissues used for immunohistochemistry were obtained from the middle portion of the regenerating intestine. This area will eventually give rise to the small intestine. We selected antibodies against ECM components of vertebrates, sea urchins, or sea cucumbers that label the interstitial matrix fibers and basal lamina of the intestine and mesentery. The antibodies used for immunohistochemistry were: (1) monoclonal 4G7 raised against basal lamina of sea urchin embryos at midgastrula (gift of Dr. E. P. Ingersoll), (2) polyclonal anti-fibronectin (SIGMA #F3648) raised against human plasma fibronectin, (3) polyclonal anti-laminin (SIGMA #L9393) raised against laminin from Englebreth Holm mouse sarcoma, (4) polyclonal antibodies (see below) raised against sea cucumber intestinal fibrous collagen, and (5) monoclonal antibody Hg-fCOL (see below) raised against sea cucumber intestinal fibrous collagen. The secondary antibodies used were FITC-labeled goat anti-rabbit and goat anti-mouse (BioSource Int., Camarillo, CA). Regenerating animals were used to analyze: (1) the thickening of the mesenteric edge, (2) the esophagus near the ruptured site, and (3) the invasion of the mucosal epithelium into the mesenteric thickenings forming the new intestinal lumen. Tissues from noneviscerated animals (small and large intestines, mesentery, and esophagus) were used as controls for comparison with the regenerating animals. Tissue sections were observed and photographed in a phase contrast and UV fluorescent microscope (Olympus IMT-2).

### Fibrous Collagen Extraction

Large intestines from *H. glaberrima* were dissected and homogenized in 1% Triton X-100 in a glass tissue grinder, and kept at −80°C until use. The homogenates were centrifuged at 1900*g* for 5 min at 4°C. The supernatant was used to determine soluble protein concentration by the Bio-Rad protein assay (Bio-Rad) and for the gel zymographs (see below). Collagen extraction was made following a modified protocol of Haralson and Hassell (1995). In brief, the pellet was resuspended in 5 ml of 0.2 M NaCl and 0.5 M acetic acid with 2 mg/ml gastric pepsin and left overnight in a shaker at 4°C. Solid NaCl was added to a final concentration of 7% (1.2 M) and shaken 4 h at room temperature. The tube was centrifuged at 1900*g* for 5 min at 4°C, the supernatant discarded, and the pellet resuspended in 2 ml of PBS 0.1 M (pH 7.4). This procedure was repeated until the pellet consisted of a white fibrous material. This insoluble fibrous

material, which is pepsin resistant, was used to immunize three Balb/c mice.

Collagen extractions for Western blots were made from noneviscerated intestines (d-0) and intestinal tissues of d-7 to d-28 regenerating animals as described above. The pellet was washed, resuspended, and centrifuged three times in PBS and then resuspended in Laemni sample buffer, 5 M urea, 20 $\mu$l/ml of 2-mercaptoethanol (in the same original volume of homogenate supernatant), and incubated at 42°C for 1 h.

## Production of Antibodies against Intestinal Fibrous Collagen

Fifty microliters of an emulsion (equal volumes of Titer Max and the extracted collagen solution) were injected intraperitoneally in each mouse. After 30 days, the serum was extracted and utilized as a polyclonal antibody source for immunohistochemistry. The sera of the three mice (fCol/Clo, fCol/Cbz, and fCol/Pos) showed similar results; a strong labeling was found against fibrous interstitial matrix and basal lamina in the sea cucumber intestine. One animal was boosted 1 week before spleen dissection and used for the production of a monoclonal antibody. The fusion was performed by the stirring method (Harlow and Lane, 1988; García-Arrarás *et al.,* 1998) with a spleen:myeloma (SP20) ratio of 10:1. The supernatant of wells exhibiting good hybridoma growth were used for immunohistochemical assays of holothuroid intestine. Cells from wells that labeled interstitial fibrous material and basal lamina were subcloned twice by limiting dilutions. From these, we selected the Hg–fCOL clone. Preimmune serum was extracted from mice and used in histological sections as a control.

## Western Blots

Collagen was extracted from tissues of noneviscerated animals (d-0) and regenerating d-7 to d-28 animals. From each sample, the equivalent volume to 30 $\mu$g of the soluble protein fraction was run in 7.5% polyacrylamide gel electrophoresis. Biotinylated broad range standards with avidin–horseradish peroxidase were used for molecular weight determination (Bio-Rad). Gels were equilibrated in Towbin transfer buffer with 15% methanol and transferred to PVDF membranes (Amersham Pharmacia Co.) in an electrophoresis transfer cell at 50 V for 2.5 h. Membranes were blocked with 5% dry milk in PBS–Tween (pH 7.4), washed in PBS–Tween, and incubated with clone supernatant Hg–fCOL (1:100). Secondary antibodies coupled to HRP (1:10,000) for ECL Plus detecting system were used as recommended by the manufacturer (Amersham Pharmacia). Band pattern was scanned, and densitometric analysis of labeled bands was performed with the Quantity One software program (Bio-Rad). Optical densitometric curves of different collagen concentrations detected in our Western blots were prepared to determine the relative differences of the extracts. Immunoblot data were analyzed by using the linear portion of the intensity/density curve.

Western blots were also made with tissue extracts treated with bacterial collagenase from noneviscerated animals to see if the molecule labeled by the monoclonal Hg–fCOL was a substrate for collagenase. Insoluble fractions from noneviscerated animals were subject to 5 ml RPMI with 2 mg/ml bacterial collagenase (SIGMA) or RPMI alone as control, incubated at 37°C for 4 h, and then analyzed in Western blots as described before.

## Gelatin and Casein Zymograph for the Detection of MMP Activities

Tissues from noneviscerated and regenerating animals (d-0 to d-28) were homogenized in 450 $\mu$l of 1% Triton X-100, then 150 $\mu$l of $4\times$ Laemni sample buffer was added to the soluble fractions for a final SDS concentration of 2.5% in non reducing conditions (no mercaptoethanol or DTT). Determination of sample protein concentration was made with the Bio-Rad protein assay reagent (Bio-Rad). For each sample, 30 $\mu$g of protein was run in electrophoresis gels made of 10% acrylamide, 1 mg/ml of collagen gelatin (porcine skin, SIGMA) or casein (SIGMA), and 0.1% SDS (modified from Haralson and Hassell, 1995; Quigley *et al.,* 1993). Electrophoresis conditions were 100 V for 1.5 h., and broad range molecular weight markers (Bio-Rad) were used for MW determination. Gels were washed in 2.5% Triton X-100 buffer solution to remove the SDS and allow proteins to renature. The gels were then incubated in 10 mM $CaCl_2$ buffer solution at 37°C overnight. To discriminate between MMPs and other proteases, duplicate of the gels were incubated with the same buffer containing the MMP inhibitor 1,10-phenanthroline (2 mM). The gels were stained with Coomassie blue to visualize translucent bands indicating gelatinolytic activities. Stained gels were scanned (GS-700 Bio-Rad) and densitometric analysis was done with Quantity One software (Bio-Rad). Optical densitometric curves were prepared from zymographies where we used different extract dilutions. Zymographic data were analyzed by using the linear portion of the intensity/density curve.

## Inhibition of MMPs during Regeneration

*H. glaberrima* specimens were eviscerated and placed in aquaria. Animals were injected in the coelomic cavity with 0.5 ml of 20 mM 1,10-phenanthroline/0.1 M PBS (pH 7.4) for an estimated final coelomic concentration of 2 mM. Animals were injected three times during the first week of regeneration (1 h after evisceration, d-2, and d-4), and dissected on d-7 for histological analysis. Control animals were injected with 0.1 M PBS (pH 7.4). Similar experiments were performed with two additional MMP inhibitors, N-CBZ-Pro-Leu-Gly hydroxamate and p-aminobenzoyl Gly-Pro-D-Leu-D-Ala hydroxamate (SIGMA). The former was injected at an estimated coelomic concentration of 0.05 mM (0.5 ml of 0.5 mM-per injection) while the latter was injected at an estimated coelomic concentration of 0.5 mM (0.1 ml of 5 mM per injection). Animals were injected on days 1, 3, and 5 of regeneration and dissected on d-7.

A second group of five experimental and five control animals received the 0.5 ml of 20 mM 1,10-phenanthroline treatment described above and were left without further injections until dissected at d-14. The purpose of this experiment was to observe whether phenanthroline-treated animals resume regenerative events after withdrawal of the drug. MMP inhibition was evaluated by measurements of the regenerating structure size and immunohistochemistry against fibrous collagen.

## Statistical Analysis

Statistical analyses using Student's *t* tests and ANOVA were made in Excel software program from Microsoft Office. Particular details of sample measurements used for the analysis are described in the corresponding figures.
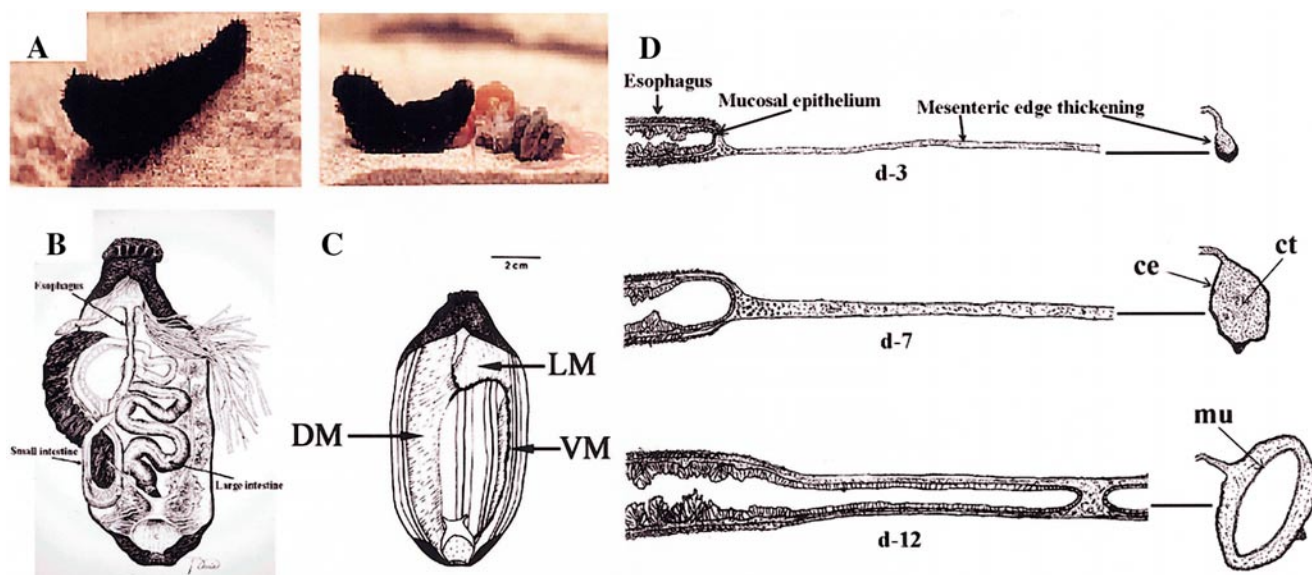
**FIG. 1.** The sea cucumber *Holothuria glaberrima* has the capacity to regenerate its internal organs following the process of evisceration. (A) Evisceration can be experimentally induced by KCl injection into the coelomic cavity. During evisceration, the intestine is detached from the esophagus, the mesenteries, and expelled through the cloaca. (B) Noneviscerated animal showing internal organs. (C) Eviscerated animal with dorsal mesentery (DM), ventral mesentery (VM), and lateral mesentery (LM). Thickening of ventral mesenteric edge initiating intestine regeneration process. (D) Diagram of longitudinal sections of the esophagus showing the mucosal epithelium tubular outgrowth and transverse sections of the mesenteric edge thickening during days 3, 7, and 12 of intestine regeneration. The tubular outgrowth of the mucosal epithelium from the esophagus invades the mesenteric edge thickening and forms the new intestinal lumen. A similar outgrowth forms in the cloaca. Abbreviations: ce, coelomic epithelium; ct, connective tissue; mu, mucosal epithelium.

## RESULTS

### Intestinal Regeneration

As previously described (García-Arrarás *et al.,* 1998, 1999), evisceration can be experimentally induced by 0.35 M KCl injection into the coelomic cavity and a new intestine is regenerated in 3–4 weeks. Animals eviscerate most of their internal organs, including small and large intestine, the hemal system, and the left respiratory tree. Evisceration causes the intestine to detach from the mesenteries and to rupture at the esophageal–intestinal junc-tion in the anterior end and at the posterior intestinal–cloaca junction. Figure 1 summarizes our findings and those reported previously from our group, necessary for the understanding of the ECM results reported in this article. *H. glaberrima* has a small and large intestine, similar in tissue structure to the vertebrate intestine. It has a coelomic epithelial lining, two muscular layers (circular and longitudinal), an inner connective tissue, and a pseudostratified mucosal epithelium. Intestinal regeneration is mainly accomplished by a thickening at the edge of the torn mesentery that includes an increase in cell density and the

**FIG. 2.** Immunohistochemistry for ECM components with the antibodies 4G7, anti-fibronectin (anti-Fn), and anti-laminin (anti-Ln) in transverse sections of the large intestine (noneviscerated) and the regenerating intestine (d-3, d-7, and d-14). (A–D) In noneviscerated animals, 4G7 labels interstitial fibers in the dense connective tissue and the basal lamina below the mucosal epithelium and muscle layers. In d-3 and d-7, the labeling can be observed in the mesentery and mesenteric thickening below the coelomic epithelium and interstitial fibers. The 4G7 sharply delineates the basal lamina of the new mucosal epithelium in the mesenteric edge by d-14. (E–H) In noneviscerated animals, anti-Fn labels irregular fibers associated to the connective tissue and the basal lamina of the mucosal epithelium. In the regenerating structure, anti-Fn labeling is prominent in the mesentery where its expression seems to be increased. (I–L) Anti-Ln only labels muscle cells in noneviscerated animals. In the regenerating tissues, anti-Ln labeling is dramatically reduced in the mesenteric edge thickenings and throughout the mesentery. Anti-Ln-labeled muscle cells become prominent at d-14 after lumen formation. Inserts are the same histological sections as seen by phase contrast. Abbreviations: ce, coelomic epithelium; ct, connective tissue; me, mesentery; ml, muscle layers; mu, mucosal epithelium. Scale bars, 100 $\mu$m.

**Large Intestine (non-eviscerated)**



© 2002 Elsevier Science (USA). All rights reserved.
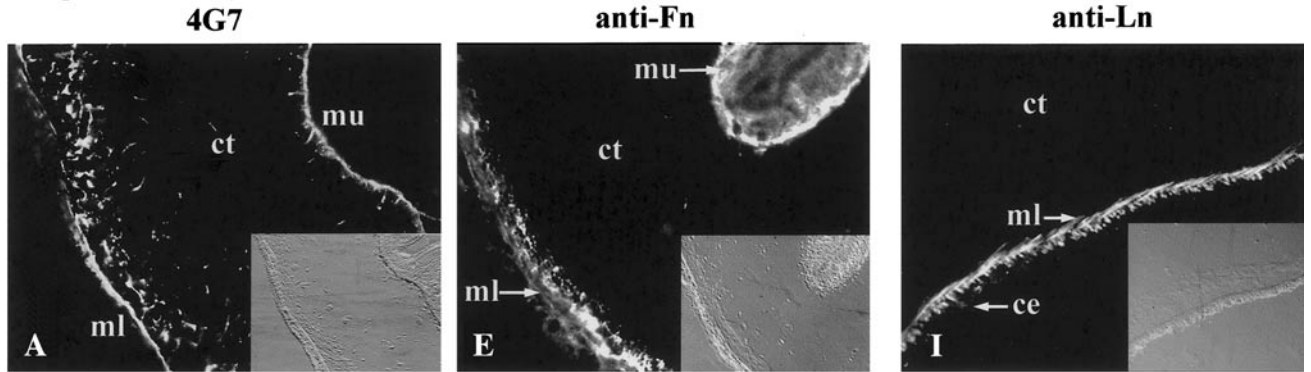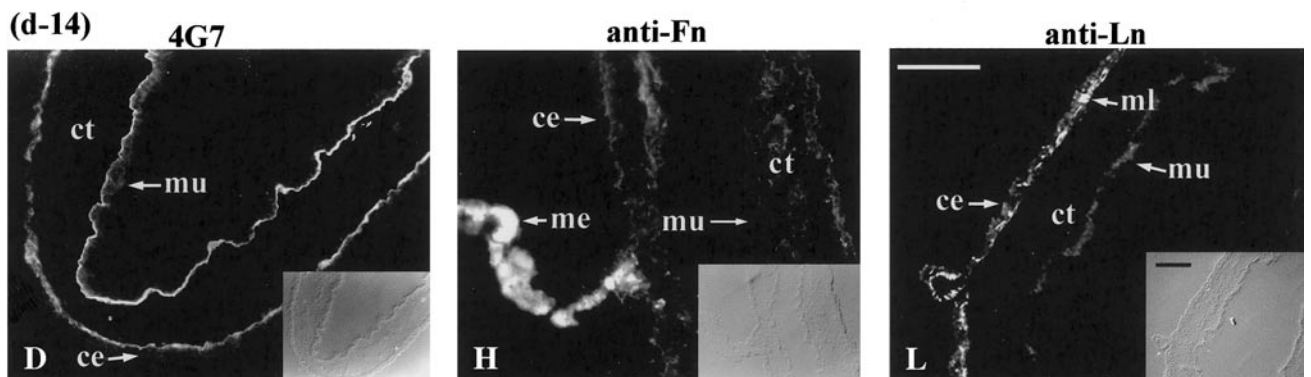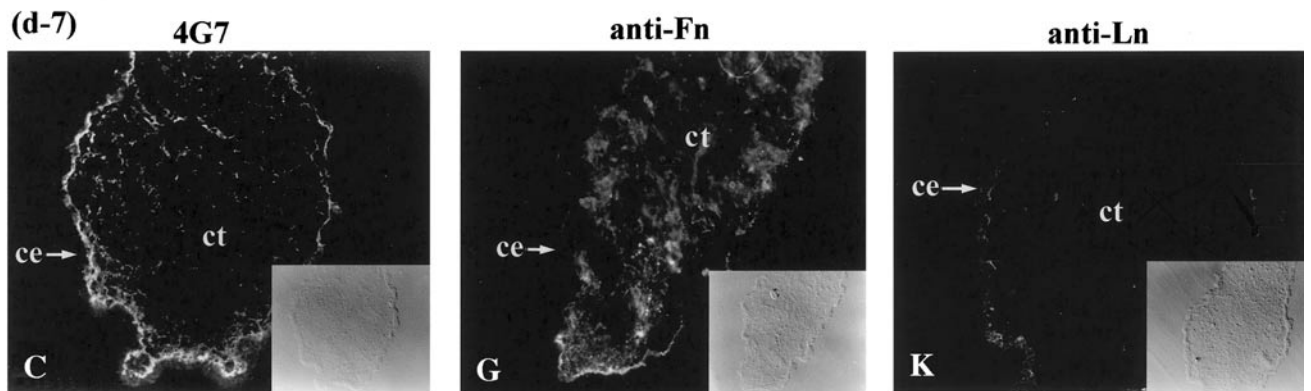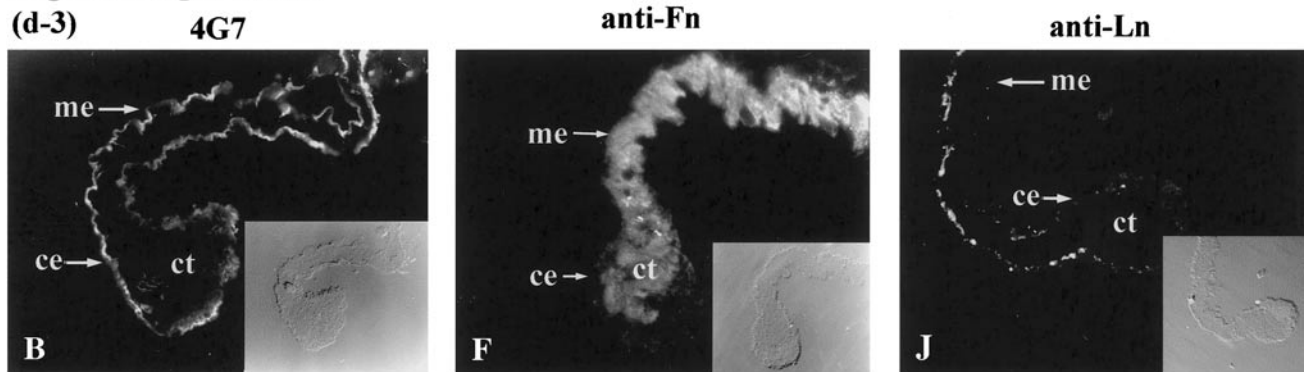
invasion of the mesenteric thickening by two tubular outgrowths of mucosal epithelia from the esophagus and the cloaca that form the new intestinal lumen.

### Immunohistochemistry against ECM Components

To observe possible changes in ECM composition and organization in the regenerating tissues, we used immuno-histochemistry with four different antibodies against ECM molecules: 4G7, anti-fibronectin, anti-laminin, and Hg-fCOL. Initial experiments were aimed at determining the presence and distribution of these ECM markers in the noneviscerated intestine of *H. glaberrima*. Once the normal expression of these ECM components was determined, these antibodies were used in histological sections of regenerating tissues. Particular attention was focused on the mesenteric edge thickening at the junction with the esophagus, where the invasion of mucosal epithelium takes place.

***4G7.***    In the intestine of noneviscerated animals, 4G7 provides a clear and distinctive labeling of two laminae: one under the mucosal epithelium, and the other under the muscle layers. In addition, 4G7 labels interstitial fibers within the inner connective tissue that protrude from both basal laminae, being most abundant and longer in the basal lamina under the muscle layers (Fig. 2A). In the mesentery, 4G7 labels a lamina under the muscle layers and dispersed interstitial fibers in the connective tissue (data not shown).

In the d-7 regenerating intestine, 4G7 labels the basal lamina below the coelomic epithelium and fibers in the new connective tissue. Rather than the observed fibrillar pattern of 4G7 labeling in the connective tissue of the noneviscerated intestine, the labeling of this molecule is observed as short fibers and dispersed granules in the regenerating intestine. By the second week, the lamina is now observed under the newly formed muscle layers and its labeling by 4G7 is now similar to that observed in noneviscerated animals (Figs. 2B–2D). In all regenerative stages, 4G7 sharply delineates the basal lamina of the new mucosal epithelium in the regenerating intestine, labeling a continuous lamina that extends from the remaining esophageal tissue to the tubular outgrowth invading the mesenteric thickening (Figs. 2D and 2B). In the mesentery of regenerating animals, the 4G7 labeling is present during the whole regeneration period in the basal lamina similar to noneviscerated animals (see Fig. 2B).

***Anti-fibronectin.***    In the intestine of noneviscerated animals, anti-fibronectin (a-Fn) labels a meshwork of interstitial matrix fibers in the inner connective tissue adjacent to the muscle layers (Fig. 2E). These fibers are thinner and form a more compact network than those labeled by 4G7. a-Fn also labels the basal lamina under the mucosal epithelium and, in the mesentery, a-Fn labels a thin fibrillar meshwork within the connective tissue.

In the regenerating animals, a-Fn can be found at all regenerative stages, however there are changes in its expression pattern. In d-7 animals, a-Fn labeling is uniformly dispersed in a diffuse and granular form in the mesenteric thickening. However, a-Fn expression is not observed in the basal lamina of the new mucosal epithelium during the first weeks of regeneration. In contrast, during the first 2 weeks, the a-Fn labeling seems to be increased in the mesentery near the regenerating structure (Figs. 2F and 2H). However, here also a-Fn labeling changes to a diffuse nonfibrillar labeling. By the third week, there is a prominent increase of a-Fn labeling in the inner connective tissue of the regenerating intestine forming a fibrillar matrix pattern that appears to be even more abundant than in noneviscerated animals (data not shown). This labeling is concentrated at two locations: below the forming muscle layers and adjacent to the mucosal epithelium.

***Anti-laminin.***    In noneviscerated and regenerating animals, anti-laminin (a-Ln) only labels the enteric and mesentery muscle cells (Figs. 2I–2L). In d-3 regenerating animals, there is no labeling within the mesenteric thickening. The labeling also disappears from the mesentery, in a gradient from the mesenteric edge thickening and moves towards the body wall. During the second week of regeneration, labeling can be detected in the regenerating muscle layer below the coelomic epithelium. In the esophagus, the a-Ln labeling also disappears in a gradient from the regenerating area towards the mouth. The disappearance of a-Ln labeling coincides with the disorganization of the muscle layers in the mesentery and esophagus during the first week of regeneration and its reappearance coincides with the reformation of the muscle layers.

***Anti-fibrous collagen.***    Sera from the three immunized mice showed similar immunoreactivity against intestinal fibrous interstitial matrix and basal lamina, while their preimmune serum was unreactive. From one of these mice the monoclonal antibody Hg-fCOL was produced.

The observed labeling pattern of the anti-collagen polyclonal and monoclonal antibodies was similar. Nonetheless, the results presented here are those obtained with the monoclonal antibody Hg-fCol. In noneviscerated animals, Hg-fCol labels a large amount of interstitial fibers as well as the basal lamina of the mucosal epithelium (Fig. 3A). The fibers are found in the inner connective tissue, with bundles of interstitial fibers running parallel to the adjacent circular muscle layer. Other fiber bundles protrude in a perpendicular pattern to the muscle layers and stretch toward the mucosal epithelium. Therefore, the collagen fiber network is heterogeneously expressed in the intestine system with a large fibrillar component within an area next to the muscle layer and a smaller fibrillar component near the mucosal epithelium. The basal lamina of the mucosal epithelium is also labeled, with short fibers running toward the connective tissue. A network of fibers is also labeled within the connective tissue of the mesentery of noneviscerated animals (not shown).

Initially, fibrous collagen fibers are present in the mesentery and mesenteric border up to d-3 (Fig. 3B). Then, a striking disappearance of collagen labeling is observed in d-7 animals (Fig. 3C). The collagen fibers are scarce or
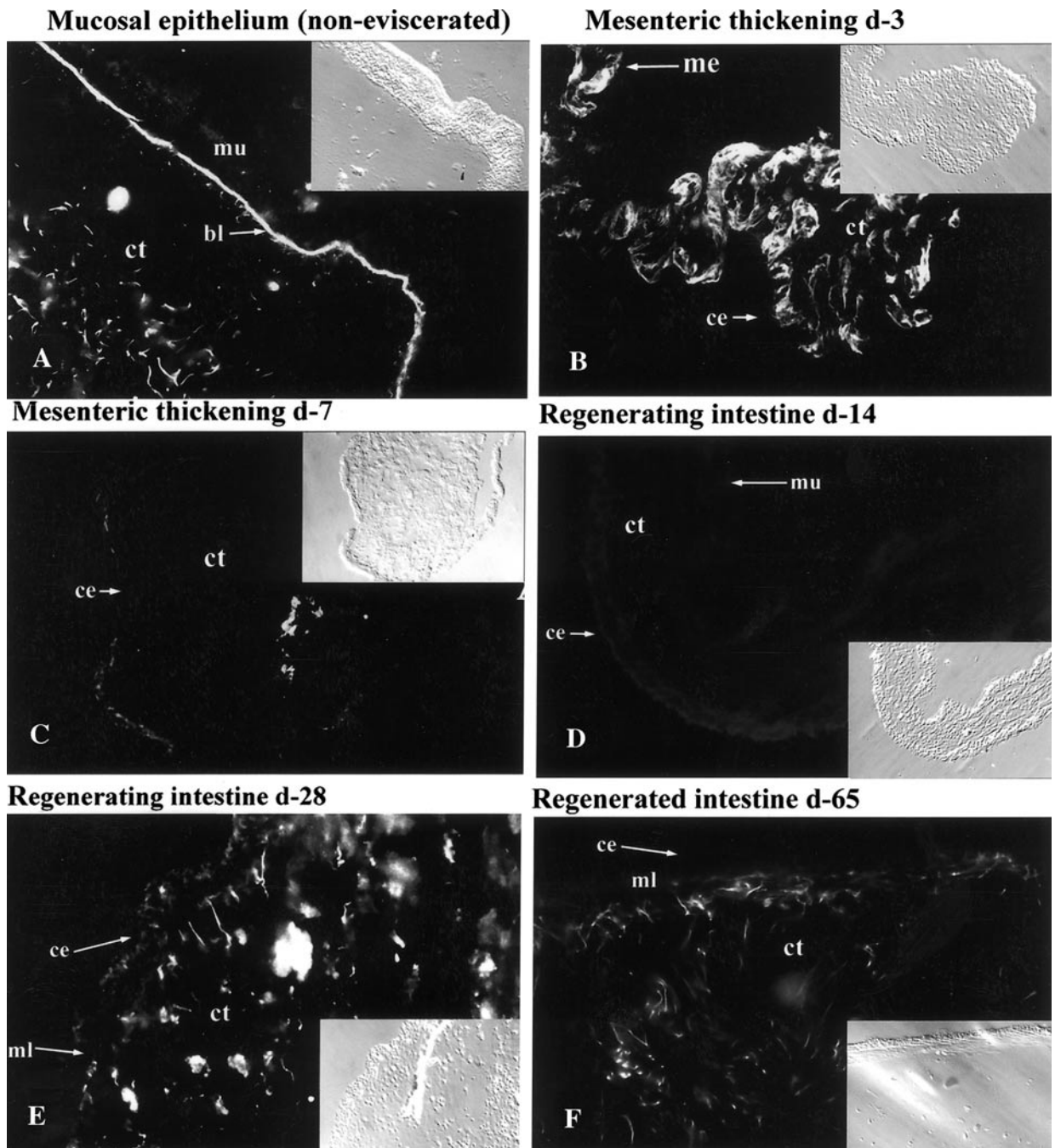
**FIG. 3.** Immunohistochemical labeling of anti-fibrous collagen by monoclonal Hg–fCOL in transverse sections of noneviscerated and regenerating intestine. (A) In large intestine of noneviscerated animals, Hg–fCOL labels collagenous interstitial fibers in the connective tissue below muscle layers, delineates the basal lamina of the mucosal epithelium, and labels fibers in the connective tissue of the mesentery. (B) At d-3, the collagen fibers are still observed in the mesentery and mesenteric edge. (C) At d-7, labeling is dramatically reduced in the regenerating intestine and in the mesentery. (D) At d-14, there is no fiber labeling in the connective tissue of the regenerating structure or in the mesentery, nor in the basal lamina of the mucosal epithelium. (E) Hg–fCOL interstitial labeling begins to appear after lumen formation as can be seen in a d-28 animal. (F) By d-65 after evisceration, the labeling is similar to that of noneviscerated intestine. Inserts are the same histological sections as seen by phase contrast visible light. Abbreviations: ce, coelomic epithelium; ct, connective tissue; me, mesentery; mu, mucosal epithelium; ml, muscle layers; bl, basal lamina. Scale bars, 100 $\mu$m.
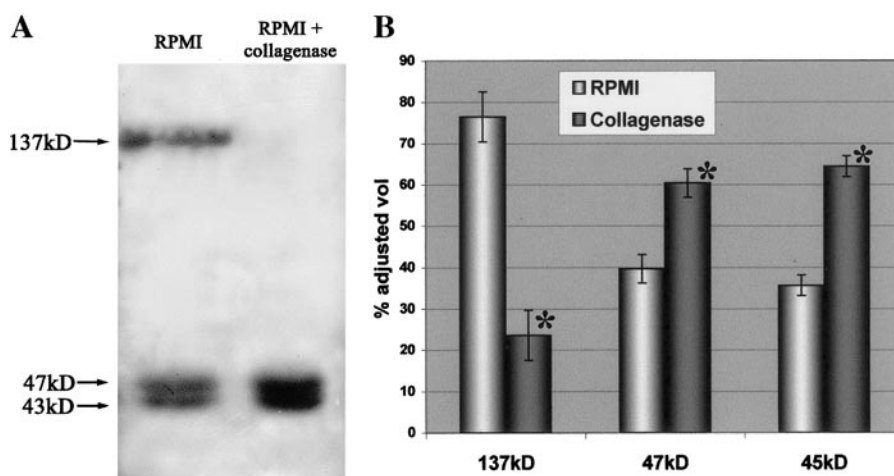
**FIG. 4.** Western blots of mesenteries from noneviscerated animals. (A) The monoclonal antibody Hg–fCOL labels a single band corresponding to 137 kDa and duplex bands corresponding to 47 and 43 kDa (lane 1). When the homogenate insoluble fraction was treated with bacterial collagenase/RPMI for 6 h at 37°C, (lane 2) the 137-kDa band disappears and the duplex bands are slightly increased. (B) Densitometric analysis of collagenase-treated homogenates vs control RPMI-treated shows that there is a significant decrease in the 137-kDa band and a corresponding increase in the band duplex. The graph represents the averages and standard errors of a total of six samples for each bar, corresponding to two Western blots from each of three different homogenates per experimental condition (*, $P < 0.01$, $n = 6$).

absent in the mesenteric thickening and throughout the mesentery segment adjacent to the regenerating structure. As one moves up the mesentery toward the body wall, the labeled fibers appear in a gradient with the largest concentration being at the most distal point from the regenerating structure. By the second week of regeneration, collagen fibers are absent in the new connective tissue and the basal lamina of the new mucosal epithelium, and have mostly disappeared from the mesentery (Fig. 3D). Collagen fibers begin their reappearance in the mesentery during the third week in a gradient that runs from the body wall toward the regenerating intestine. By the fourth week, fibers are found within the regenerating intestine, in the connective tissue below the muscle layers, but these are not as abundant as in noneviscerated intestine. At this stage, the basal lamina of the mucosal epithelium is still not labeled (Fig. 3E). In animals at d-65, there is an abundant increase of collagen interstitial fibers in the connective tissue of the regenerated organ and the mesentery, similar to what is found in noneviscerated intestines (Fig. 3F). At this stage, collagen labeling in the basal lamina of the mucosal epithelium has reappeared in some animals.

A similar disappearance of collagen labeling can be found in the esophagus of regenerating animals; by the first week, the presence of the interstitial fibers, as well as the labeling of the basal lamina disappears in a gradient that runs from the regenerating area towards the mouth. Labeling is also absent in the basal lamina of the mucosal epithelium tubular outgrowth that is beginning to invade the mesenteric thickening. By the third week, collagen fibers begin to reappear and increase in concentration near the regenerating area, which already has a newly formed lumen.

### Western Blots to Determine Fibrous Collagen Content

Pro-collagens and collagens can be identified on gels as bands that disappear when samples are treated with purified bacterial collagenase prior to electrophoresis (Haralson and Hassell, 1995). Therefore, our initial Western blots were made to determine that the molecule labeled by Hg–fCOL is indeed a substrate for a bacterial collagenase. In homogenates of noneviscerated mesentery (d-0), the monoclonal Hg–fCOL labels a 137-kDa band and duplex bands of 47 and 43 kDa. When the extract was pretreated with bacterial collagenase, the density of the 137-kDa band is significantly decreased, while the density of the duplex bands is increased (Figs. 4A and 4B).

Western blots were also made to quantify the changes in fibrous collagen content during regeneration and correlate these changes with the immunohistochemical data. Homogenates from noneviscerated mesentery (d-0) and from mesentery with the regenerating structure (d-7, d-14, d-21, and d-28) were used. These results show that the overall fibrous collagen content in the regenerating tissues decreases significantly during the first 2 weeks of regeneration as compared with noneviscerated (d-0) mesenteric tissues. Densitometric analysis of horizontal scanned bands of Western blots shows that, by the second week of regeneration, the 137-kDa band decreased fivefold and the duplex
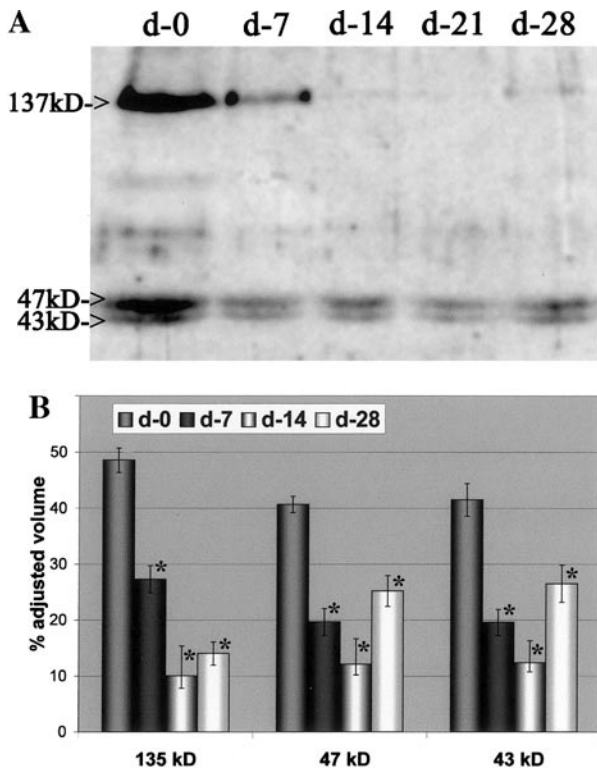
**FIG. 5.** (A) Western blots for the detection of relative collagen content as detected by monoclonal Hg–fCOL in homogenates from noneviscerated mesentery (d-0), mesenteric thickening, and regenerating intestine (d-7, d-14, d-21, and d-28). (B) Relative changes in collagen content of regenerating and noneviscerated animals. Densitometric analysis of a horizontal scanned area corresponding to the single and duplex bands show that the collagen content decreases significantly during the first 2 weeks after evisceration. Results represent the mean ± SE of six different Western blots, corresponding to two blots from each of three different homogenates per experimental condition (*, $P < 0.01$ as compared with d-0, $n = 6$).

bands (47 and 43 kDa) decreased near fourfold when compared with noneviscerated mesentery (Figs. 5A and 5B). After the fourth week of regeneration, the collagen content of these tissues is slightly increased as compared with d-14. Thus, the observed decrease of fibrous collagen content during regeneration in Western blot analysis parallels the decrease in fibrous collagen observed in histological sections with immunohistochemistry.

### Zymography for MMP Activities

Since ECM degradation is an initial step of tissue repair in vertebrates, we made collagen–gelatin and casein gel zymographs to detect MMP proteolytic activities in intestinal tissue homogenates. In collagen gel zymography of mesenteric tissue samples from noneviscerated animals (d-0), we

have identified at least four consistent gelatinolytic bands corresponding to the 59, 51, 45, and 43 kDa (Fig. 6A). All these bands are sensitive to the MMP inhibitor 1,10-phenanthroline showing that they are zinc-dependent metalloproteinases (Fig. 6B). These bands are not inhibited by other proteases inhibitors, such as pepstatin-A and benzamidine (data not shown). In addition, no proteolytic activity
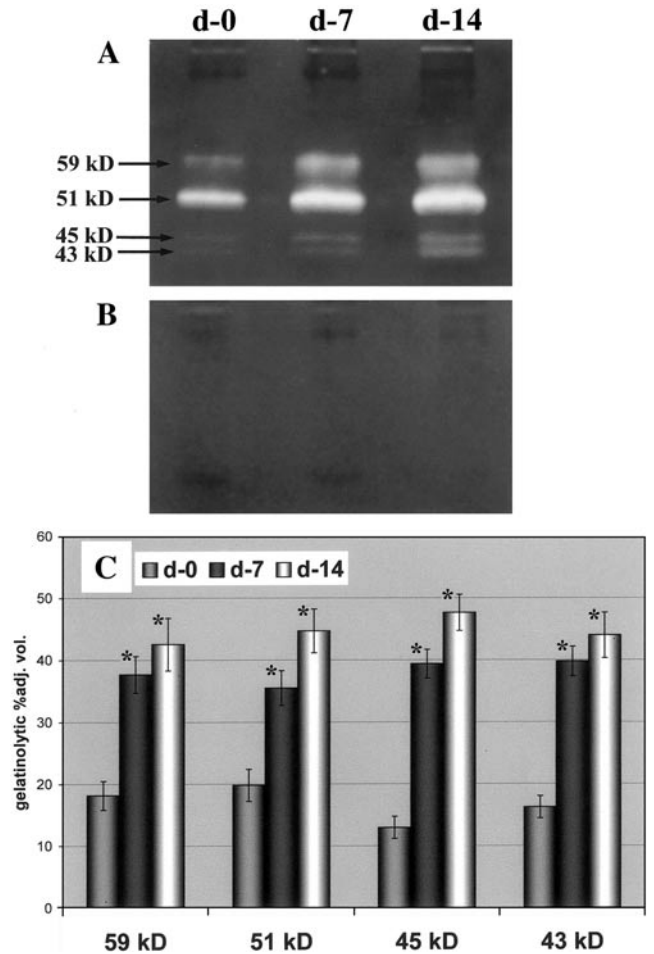


**FIG. 6.** Zymograph for the analyses of MMPs gelatinolytic activities in homogenates from noneviscerated mesentery (d-0) and mesenteric thickenings during regeneration (d-7 and d-14). (A) Four bands of gelatinolytic activities are consistently detected in all zymographs corresponding to the 59, 51, 45, and 43 kDa. (B) Zymograph of a gel incubated in the presence of the MMPs inhibitor 1,10-phenanthroline (2 mM), showing that these bands are zinc-dependent gelatinases. (C) Densitometric analysis of horizontally scanned bands shows that the gelatinolytic activities of d-7 and d-14 homogenates are significantly higher than that of noneviscerated mesentery. Results represent the mean ± SE of 12 different zymographs, corresponding to 4 zymographs from each of 3 different homogenates per experimental condition (*, $P < 0.01$ as compared with d-0, $n = 12$).

was detected in casein gel zymographs of noneviscerated or regenerating tissues (data not shown).

Collagen–gelatin gel zymographs were made from homogenates of noneviscerated (d-0) mesenteries and regenerating tissues (d-7 and d-14) to determine relative changes in activities during regeneration. Densitometric analysis revealed an increase in the activity of the four bands during the first 2 weeks of regeneration when compared with noneviscerated mesenteries (d-0) (Fig. 6C). This increase parallels the decrease in fibrous collagen matrix observed with immunohistochemistry and Western blots. After the second week of regeneration, other bands with proteolytic activity appeared. However, these were not phenanthroline-sensitive and may be digestive enzymes of the new mucosal epithelium, since they are also observed in noneviscerated intestinal homogenates (data not shown).

### Inhibition of MMPs during the Onset of the First Stages of Intestine Regeneration

The enhanced gelatinolytic activity observed during early regenerative stages suggest that MMPs may play a role in the observed ECM changes. To determine whether MMP activities are critical for the onset of the regenerative events, we performed inhibition experiments in regenerating animals. Intracoelomic injections with 1,10-phenanthroline were done in experimental animals and compared with a control group injected with 0.1 M PBS (pH 7.4). Phenanthroline-treated animals were found to be delayed in their regeneration program. This delay was on the order of about 4–6 days and could be detected by impaired early regenerative events such as: a smaller size of the mesenteric thickening, a shorter mucosal epithelium outgrowth from the esophagus, and reduced fibrous collagen disappearance. Measurements of the mesenteric thickenings in the histological sections show that phenanthroline-treated animals have a regenerating structure ten times smaller than PBS-treated animals (Fig. 7). Also, 1 week following evisceration, PBS-treated animals had the mucosal tubular outgrowth already extending from the esophagus into the mesenteric thickening. This was not observed in phenanthroline-treated animals where the tubular outgrowth is still in or near the esophagus area. Finally, histological observations at d-7 show that, in PBS-treated animals, the Hg–fCOL labeling in the mesenteries and regenerating structures has mostly disappeared, while in phenanthroline-treated animals, the collagen labeling is still present in the mesenteries and in the regenerating structure (not shown).

To exclude the possibility that the phenanthroline effects were due to toxic or lethal effects on the regenerating tissues, a group of phenanthroline-treated and PBS-treated animals were not dissected on day 7 but were left without further injections up to day 14. Histological sections of these animals showed that phenanthroline-treated animals, although with a lag in their regenerative stage, had indeed resumed regeneration (Fig. 8). Their regenerating structures

were closer in size to those of a d-8 or d-10 animal instead of the d-14 size shown by PBS-treated animals. In the d-14 phenanthroline-treated animals, the invasion of the mucosal epithelium into the mesenteric thickenings proceeded forming the new intestinal lumen equivalent to d-8 or d-10 control animals. Also, the Hg–fCOL labeling of fibrous collagen in these experimental animals had disappeared from the mesenteries and regenerating structures as occurred in control animals.

Nevertheless, phenanthroline is a broad-range inhibitor that could be exerting an effect on regeneration processes other than those mediated by MMPs. To narrow the regeneration effect to the MMPs, we repeated the experiments but this time using specific MMP inhibitors. Two such inhibitors were used, the peptidyl hydroxamic acids: N-CBZ-Pro-Leu-Gly hydroxamate and p-aminobenzoyl Gly-Pro-D-Leu-D-Ala hydroxamate. Both are known to bind to the enzyme, causing a competitive inhibition and displacing the natural substrate from the enzyme active site. Both inhibitors caused effects similar to those observed after phenanthroline treatment, mainly, an inhibition of intestinal regeneration as viewed by a decrease in the size of the regenerating structure (Fig. 9) and reduced fibrous collagen disappearance as detected by immunohistochemistry (not shown). Nonetheless, the magnitude of the effect caused by the two inhibitors differed. N-CBZ-Pro-Leu-Gly hydroxamate caused a pronounced inhibition in the size of the regenerating structure to about 33% of the controls, while p-aminobenzoyl Gly-Pro-D-Leu-D-ala hydroxamate caused only a small decrease in the size of the regenerating structure to about 71% of the controls.

## DISCUSSION

### ECM Labeling in the Intestine of Noneviscerated Holothuria glaberrima

We have identified four ECM components within the connective tissue of the holothuroid intestine and mesentery. Each component is recognized by a particular antibody and shows a unique pattern of labeling in terms of fiber characteristic, abundance, or localization. Thus, in terms of the goals of the present experiments, we expect to be labeling four different ECM components: fibrous collagen, fibronectin, laminin, and a yet unidentified echinoderm ECM component. However, at least three of these components are made up of a family of closely related molecules or isoforms, and therefore each antibody is probably labeling one or a subset of the members of the particular ECM molecule family. For example, in vertebrates, the fibronectin family contains at least eight splice variants, and laminins have at least nine genetically distinct subunits and several isoforms (Schwarzbauer, 1991, Kreis and Vale, 1994; Haralson and Hassell, 1995). Nevertheless, the expression pattern, the comparison to what is known of ECM molecules in other metazoans and the available information on the production of the antibodies themselves, provide im-
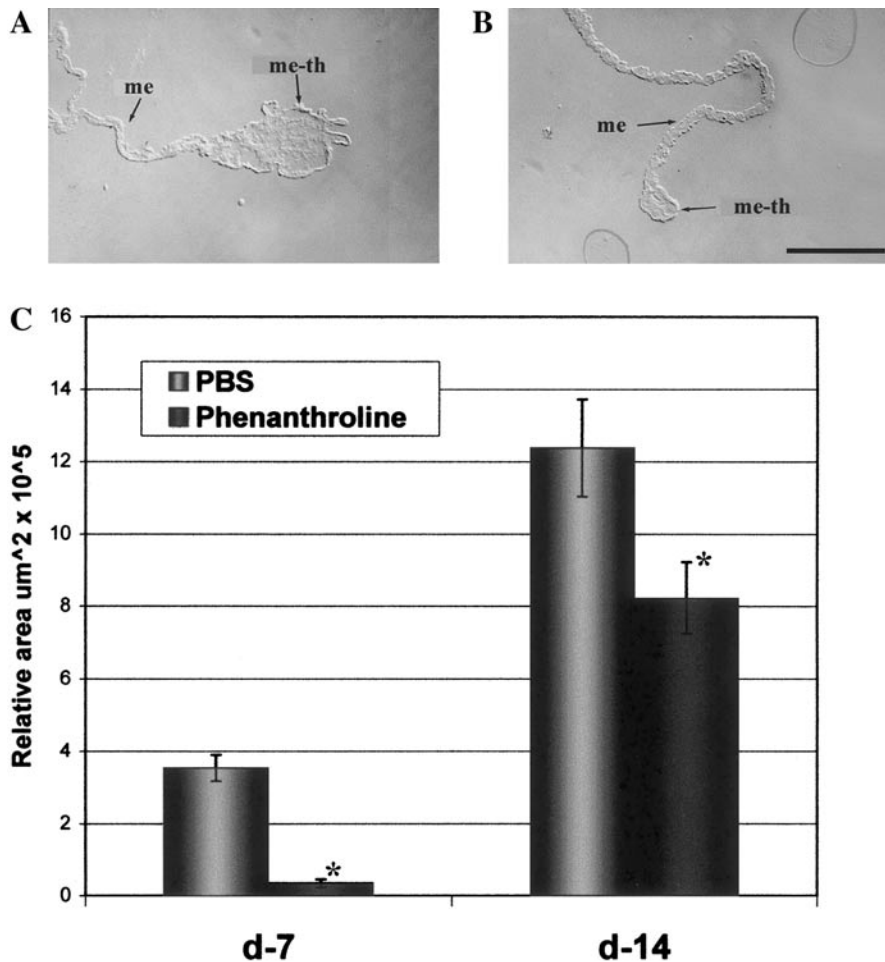
**FIG. 7.** Intracoelomic injections of MMPs inhibitor, 1–10,phenanthroline, delay early regenerative events. (A, B) Histological observations of d-7 animals show that the mesenteric edge thickening in the PBS injected animals (A) has the characteristic size of a normal regenerating structure, while in phenanthroline-treated animals (B), it is significantly reduced in size. (C) Measurements of the relative area of the thickenings show a 10-fold decrease in the mesenteric thickening size of phenanthroline-treated animals as compared with PBS controls (*, $P < 0.01$, $n = 4$). By d-14, even though no further injections were made, the size of the regenerating intestine of phenanthroline-treated animals still lagged behind that of PBS-treated animals. Abbreviations: me, mesentery; me-th, mesenteric thickening. Scale bars, 500 $\mu$m.

portant information on the possible molecules identified by immunohistochemistry within the holothuroid intestine.

Members of the fibronectin family are known to be temporally and spatially expressed during intestinal development in vertebrates. Fibronectin is initially detected as a linear band at the endodermal/mesenchymal interface during embryonic development, and in adults, is also localized in the muscle layers in narrow spaces between the muscle cells (Simon-Assmann, 1995; Kurisu *et al.,* 1987). In noneviscerated intestines of *H. glaberrima*, the a-Fn also labels the basal lamina of the mucosal epithelium, but instead of being present between the muscle cells, the a-Fn is abundantly present in a meshwork of interstitial fibers below the muscle layer in the connective tissue. Antibodies against human plasma fibronectin have also been used for studies

on basal lamina ontogeny during early embryogenesis of the sea urchin *Lytechinus variegatus* (Wessel *et al.,* 1984). In this case, fibronectin has also been associated with the basal lamina of the developing embryo (blastula to pluteus larva) and with the migrating primary mesenchyme.

In vertebrates, various laminin isoforms have been identified within the intestinal ECM (Simon-Assmann *et al.,* 1995; Simo *et al.,* 1991). Laminin-l has been localized to the basal lamina of the mucosal epithelium and the muscle layers as well as to the connective tissue of the submucosa. Laminin-3 is solely localized on the muscle layers, and laminin-2 and -5 are only found in the basal lamina of the mucosal epithelium. The laminin antibody used in our studies is a polyclonal raised against laminin-l from Englebreth Holm mouse sarcoma. Nevertheless, in the holothu-
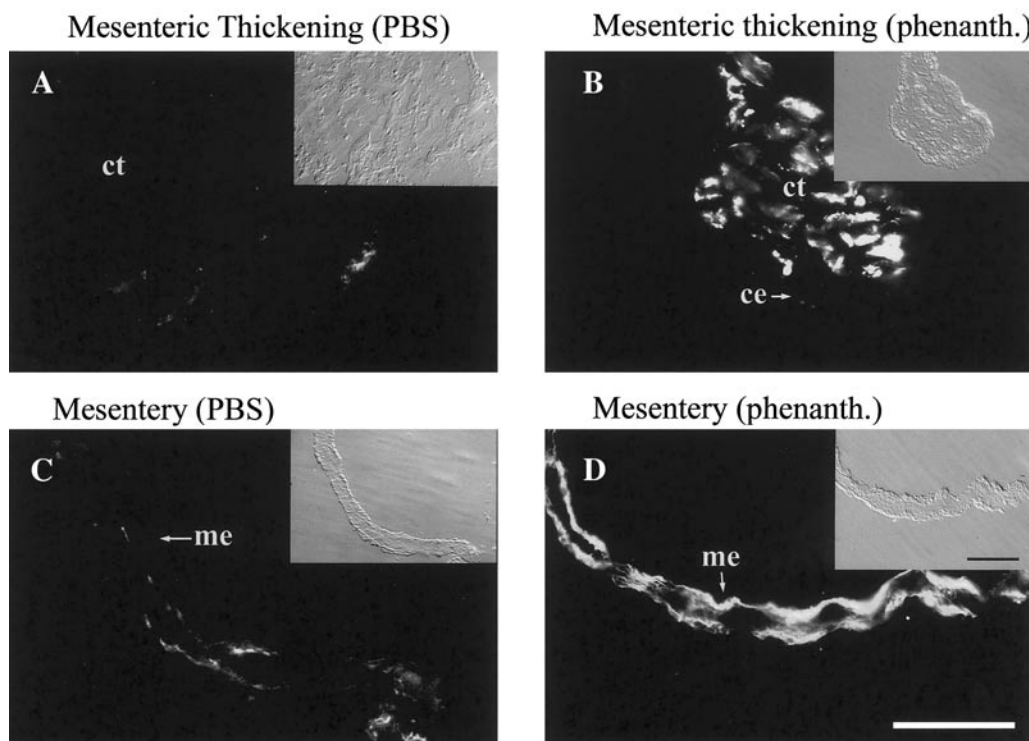
**FIG. 8.** Effects of intracoelomic injections of MMPs inhibitor 1–10,phenanthroline on fibrous collagen expression in the thickening of the mesenteric border and the mesentery of regenerating animals. (A, C) Fibrous collagen labeled by monoclonal Hg–fCOL is absent from the d-7 mesenteric edge thickening and mesentery of PBS treated animals but is present in the d-7 mesenteric edge thickening and mesentery of most phenanthroline-treated animals (B, D). Scale bars, 100 $\mu$m.

roid, it appears to be identifying a muscle-specific laminin isoform. It is obvious that further experimentation is necessary to define the laminin component of the holothuroid intestine.

The ECM component identified by 4G7 has not been characterized, but from the spatial and temporal localization, it appears to differ from the other labeled components. The monoclonal 4G7 was raised against sea urchin embryonic connective tissue and its spatial labeling pattern in *H. glaberrima* is similar in some aspects to that of anti-fibrous collagen. Nevertheless, the differences in the organization and temporal expression during regeneration show that this antibody labels a different type of interstitial fibers from those labeled by collagen antibodies.

In contrast to the unknown nature of the 4G7 labeling, the molecule recognized by the collagen anti-sera and monoclonal supernatants is a fibrous collagen. Two main characteristics of collagen molecules were used with salt fractionation steps to extract and isolate fibrous collagen to obtain the material for antibody production: (1) the post-translational covalent cross-linking between the subunits that makes these molecules highly insoluble, and (2) the triple helical subunits structure that confers resistance to gastric pepsin (Haralson and Hassell, 1995). Also, collage-

nase experiments show that the molecule is a substrate for bacterial collagenases. Previous studies have shown that fibrous collagen extracted from sea cucumber dermis and cuvierian tubules by pepsin digestion and a salt fractionation step (NaCl 1.2 M) has a similar amino acid composition to mammalian type I collagen (Bailey, 1984). In addition, the banding pattern observed in Western blots is similar to the holothuroid collagen identified as type I (Bailey, 1984). In the vertebrate intestine, the expression of type I and III fibrous collagen (protein and mRNA) is restricted to the submucosal connective tissue, collagen I being the most abundant (Sanberg *et al.,* 1989, Simon-Assmann *et al.,* 1995). In *H. glaberrima*, fibrous collagen labeling is also observed in the inner connective tissue between the mucosal epithelium and the muscle layers, and is not detected in the muscle layers. In contrast to vertebrate intestine, this molecule is also present in the basal lamina of the mucosal epithelium.

### Changes in ECM Composition Reflects Matrix Remodeling during Intestine Regeneration

We have observed changes in ECM components during intestinal regeneration as compared with their expression
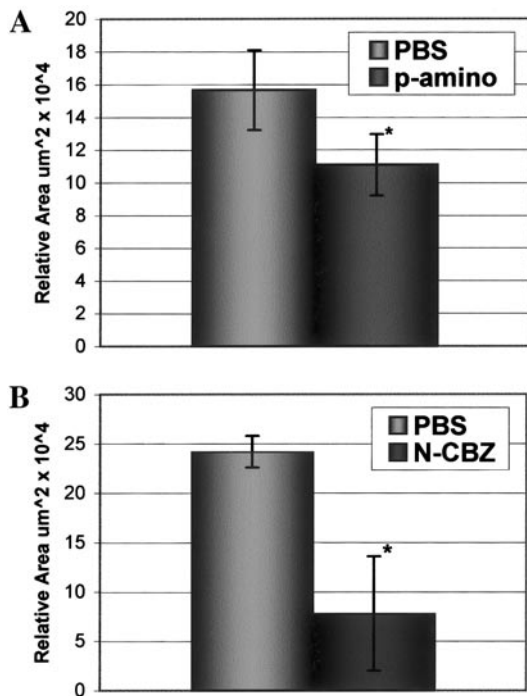
**FIG. 9.** Intracoelomic injections of specific MMPs inhibitor delays early regenerative events. Measurements of the relative area of the thickenings show a decrease in the mesenteric thickening size of p-amino Gly-Pro-D-Leu-D-Ala hydroxamate- (A) and N-CBZ-Pro-Leu-Gly hydroxamate-treated (B) animals as compared with PBS controls (*, $P < 0.05$; (A) $n = 8$, (B) $n = 6$).

pattern in noneviscerated intestine and mesentery. These changes can vary depending on the ECM component: some molecules apparently disappear from the basal laminas and/or matrix interstitial fibers, and other molecules are present at all time showing slight changes in their expression pattern. Laminin and fibrous collagen are examples of molecules whose expression disappear, while fibronectin and 4G7 are the ones with continuous expression that undergoes slight changes.

The selective pattern of expression of the ECM molecules during regeneration is best exemplified by 4G7 and fibrous collagen. 4G7 labeling delineates the basal lamina of the coelomic epithelium in the regenerating structure and mesentery, as well as the luminal epithelium basal lamina, at all regenerative stages. This is important since it implies that a basal lamina structure is continuously present during the tubular epithelial outgrowth and the molecule labeled by 4G7 is continuously synthesized and accumulated in this growing structure during lumen formation. The same occurs with the basal lamina under the coelomic epithelium in the newly formed regenerating structure. In contrast anti-fibrous collagen (Hg–fCOL) labeling disappears from the same location in the basal lamina and interstitial

matrix during early regenerative stages, and its reappearance is temporarily delayed.

Fibronectins are high molecular weight glycoproteins found in many extracellular matrices in the interstitial matrix and basal lamina of epithelia. These molecules have binding sites for other extracellular molecules, such as a gelatin collagen and a heparan sulfate, which could mediate matrix–matrix or cell–matrix interactions (Kreis and Vale, 1994). It is possible that the observed fibronectin changes in the mesentery at early regenerative stages could be related to the disorganization of the collagen matrix. Thus, following the disappearance of collagen molecules, the observed fibrillar network of fibronectin becomes disorganized. Nevertheless, changes in the fibronectin content and fibrillar organization in the mesentery and regenerating intestine may play a role during regeneration, similar to the role it plays during other regenerative events such as the epithelial restitution in vertebrate wounded skin (Rooney and Kumar, 1993; Martin, 1997), *in vitro* intestine epithelial restitution (Goke *et al.,* 1996), *in vitro* alveolar epithelial restitution (Garat *et al.,* 1996), and newt limb regeneration (Nace and Tassava, 1995; Christensen and Tassava, 2000).

Fibronectins also have cell-binding sites that promote cell adhesion and are known to affect morphology, migration, and differentiation. In particular, the role of fibronectin during cell migration and development has been widely documented. Fibronectin has been shown to be involved in the migration of vertebrate neural crest cells (Bronner-Fraser, 1986, 1993), cortical neurons (Sheppard *et al.,* 1991, 1995), and mesenchymal cells in sea urchins (Spiegel *et al.,* 1983; Wessel *et al.,* 1984). Cell migration via the mesentery into the mesenteric thickening has been proposed to occur during holothuroid regeneration (García-Arrarás *et al.,* 1998). When the mesenteric edge increases in size, there is a concomitant increase in cell density within the inner connective tissue which is not due to proliferation. Thus, it is possible that these cells are migrating through the mesenteric connective tissue and that the ECM remodeling described here, particularly changes in fibronectin, may play an important role in this migration.

In vertebrate skin, during wound healing and restitution of tissues, the collagen matrix is degraded and a temporary matrix is formed, consisting primary of hyaluronic acid, fibronectin and fibrin (Rooney and Kumar, 1993; Martin, 1997). After restitution of tissues, the hyaluronic acid is degraded, and the collagen matrix is resynthesized and accumulated. Collagen matrix remodeling also occurs during wound healing and restitution of tissues after induction of gastric ulcers (Pohle *et al.,* 1997). In both skin and gastric wound healing, the reposition of fibrous collagen is initiated 3–4 days after the lesions have occurred (Rooney and Kumar, 1993; Pohle *et al.,* 1997). Similarly, our results imply a disappearance of fibrous collagen within the ECM in the early stages of regeneration showing a dramatic change in fibrous collagen expression as documented by immunohistochemistry and Western blots. In contrast to vertebrates, the reappearance of fibrous collagen in *H.*

*glaberrima* is observed relatively late during regeneration (d-21). Collagen reappearance is preceded by other events, such as the formation of a new lumen and muscle layers, forming a new intestine that appears to be functional. This delayed reappearance of fibrous collagen seems to be a key aspect of the regenerative events and could account for the impressive regenerative capacities of echinoderms.

Fibrillar collagen resorption has also been reported during wound healing and regenerative events in other holothuroids. Ultrastructure description of cuvierian tubule regeneration in the sea cucumber *H. forskali* revealed that the first three stages of regeneration (d-0 to d-14) are characterized by the poor presence of collagen fibers in the connective tissue, where phagocytes containing large secondary lysosomes enclosing partly decomposed collagen fibrils were observed (VandenSpiegel *et al.,* 2000). Only after small tubules have reformed and begin to increase in size (d-14 to d-21) are collagen fibers observed to increase in quantity.

Our immunohistochemical results show that ECM remodeling occurs during intestine regeneration in *H. glaberrima*, in the mesentery, the esophagus, and the regenerating structure. The disappearance of some ECM molecules is not a direct effect of tissue tearing during evisceration, but a gradual selective removal of these components during the first stages of regeneration and a selective temporal reposition of these components. Normal matrix composition begins to be reestablished after the animal has formed a new intestine.

### Matrix Metalloproteinases Play a Critical Role in the Onset of Intestine Regeneration

ECM remodeling during regeneration has been associated with the proteolytic activities of the metalloproteinases (MMPs). In *H. glaberrima,* the observed ECM remodeling during intestine regeneration appears to be directly related to the MMP activities. In fact, the observed increase in MMP gelatinolytic activities coincides with the decrease of fibrous collagen in tissues, as seen by immunohistochemistry and Western blot analysis. Similarly, in rats, intestinal MMPs and ECM remodeling have been associated with the repair of intestinal wounds produced by surgical procedures or irradiation (Seifert *et al.,* 1996, 1997). In experiments where lesions to the ileum and colon of rats were made, various gelatinolytic phenanthroline sensitive bands were detected in zymographs and the overall activity of these MMPs increased during the first 3 days postsurgery. Increased activities of MMPs during wound healing and regeneration have also been reported during other regenerative events, such as, regeneration of newts' limb (Yang and Bryant, 1994; Miyazaki *et al.,* 199; Park and Kim, 1999), *Xenopus* wound healing (Carinato *et al.,* 2000), mammalian hepatic tissue repair (Haruyama *et al.,* 2000; Knittel *et al.,* 2000), regeneration in *Hydra* (Yan *et al.,* 2000a, 2000b), regenerating skeletal muscles (Kherif *et al.,* 1999), and human wounded respiratory epithelium (Buisson *et al.,* 1996).

The association between ECM remodeling, MMP activities, and regenerative events is further strengthened by the *in vivo* MMP inhibition experiments. Inhibition of MMPs by two types of inhibitors, with different sites of action, causes a decrease in ECM remodeling and in intestinal regenerative events as shown by the persistent presence of fibrous collagen in the mesentery and a decrease in the thickening of the mesenteric edge. Phenanthroline works by removal of the zinc ion, while peptidyl hydroxamic acids form a ternary complex with the enzyme, binding to the active site (Moore and Spilburg, 1986b). The two hydroxamic acid competitive inhibitors show different effectiveness which might be due to their affinity for the enzyme. P-aminobenzoyl Gly-Pro-D-Leu-D-Ala hydroxamate causes a smaller inhibition of regeneration than N-CBZ-Pro-Leu-Gly hydroxamate. In contrast, in experiments with human fibroblast collagenase, P-aminobenzoyl Gly-Pro-D-Leu-D-Ala hydroamate was found to be a more effective inhibitor ($IC_{50} = 1$ $\mu$M) (Odake *et al.,* 1994) than N-CBZ-Pro-Leu-Gly hydroxamate ($IC_{50} = 40$ $\mu$M) (Moore and Spilburg, 1986a). Thus, it is possible that the most effective inhibitor of human collagenase being highly specialized to recognize the active site of the human enzyme, recognizes less well the holothurian enzyme.

After withdrawal of the inhibitor in experimental animals, the inhibited regenerative events are resumed (at least for 1,10-phenanthroline), showing that the effect is reversible. Our experiments coincide with results obtained in sea urchin where the inhibitors 1,10-phenanthroline, TIMP-2, and BB-94 have been used to determine the possible role of MMPs during development. Inhibition of MMPs after archenteron formation inhibits spiculogenesis in *S. purpuratus* and the effect of 1,10-phenanthroline is reversible (Roe *et al.,* 1989; Ingersoll and Wilt, 1998). Therefore, our data show that MMP activities during regeneration are critical for the onset of the first regenerative stages.

### Fibrosis vs Regeneration?

When skin lesions are made in adult vertebrate, they lead to scarring and fibrotic tissue (Rooney and Kumar, 1993; Martin, 1997). In contrast if the lesions are made to human or sheep fetal skin, no fibrotic tissue or scarring appears. In the fetal tissues, wound healing is characterized by an increase in interstitial collagenases, gelatinase A and stromelysin-1, and a difference in the distribution and deposition of fibrous collagens as compared with adult skins (Bullard *et al.,* 1997; Lovvorn *et al.,* 1999). In contrast to the regenerative capacity of fetal skin, wounded intestines in vertebrates produce scarring and fibrotic tissue in both, fetal and adult intestines (Meuli *et al.,* 1995; Mast *et al.,* 1998). Different from the fibrosis formation in adult vertebrates, in the mesentery and regenerating intestine of *H. glaberrima*, we do not observed signs of scarring or fibrotic tissues in the wounded areas during or after regeneration.

It seems that the excessive fibrosis that impairs the

restitution of tissues in vertebrates is associated with fibrous collagen deposition and the regulation of metalloproteinases. In fact, induction of MMP activities help in reducing or preventing hepatic and myocardial fibrosis (Haruyama *et al.,* 2000; Taniyama *et al.,* 2000). On the other hand, MMP inhibition leads to fibrosis and scar formation in fetal skin tissues as occurs in adult skin (Lin *et al.,* 1995; Bullard *et al.,* 1997). Fibrosis in adult wounded skin can be significantly reduced if MMP inhibition is prevented (Roony and Kumar, 1993; Choi *et al.,* 1996; Martin, 1997; Brahmatewari *et al.,* 2000). Similarly, when MMP activities are inhibited during intestine regeneration in *H. glaberrima,* collagen matrix persists and the regenerative events are impaired. Thus, the regenerative capacity of *H. glaberrima* associated with ECM remodeling, in particular with collagen matrix degradation, could also be associated with the delayed deposition of fibrous collagen.

In *H. glaberrima*, developmental events such as wound healing, restitution of tissues, and tubular epithelial outgrowth occur during intestine regeneration. The capacity to regenerate a whole organ in holothuroids could be associated with the dynamics of ECM changes and the regulation of MMP activities. The present work, for the first time, provides evidence that extracellular matrix remodeling occurs during whole organ regeneration in *H. glaberrima* and that MMP activities are a critical step for the onset of intestinal regeneration.

## ACKNOWLEDGMENTS

## REFERENCES

Adams, J. C., and Watt, F. M. (1993). Regulation of development and differentiation by the extracellular matrix. *Development* **117,** 1183–1198.

Ashkenas, J., Muschler, J., and Bissell, M. J. (1996). The extracellular matrix in epithelial biology: Shared molecules and common themes in distant phyla. *Dev. Biol.* **180,** 433–444.

Bai, M. M. (1971). Regeneration in the Holothurian, *Holothuria scabra jager. Indian J. Exp. Biol.* **9,** 467–471.

Bailey, A. J. (1984). The collagen of the echinodermata. In "Biology of Invertebrate and Lower Vertebrate Collagens" (A. Bairati and R. Garrone, Eds.). pp. 369–388. Plenum Press, New York.

Belloch, R., and Kimble, J. (1999). Control of organ shape by a secreted metalloprotease in the nematode *Caenorhabditis elegans. Nature* **399,** 586–590.

Brahmatewari, J., Serafini, A., Seralta, V., Mertz, P. M., and Eaglstein, W. H. (2000). The effects of topical transforming growth factor-b2 and anti-transforming growth factor-b2, 3 on scarring in pigs. *J. Cutan. Med. Surg.* **4,** 126–131.

Bronner-Fraser, M. (1986). An antibody to a receptor for fibronectin and laminin perturbs cranial neural crest development in vivo. *Dev. Biol.* **117,** 528–553.

Bronner-Fraser, M. (1993). Mechanism of neural crest cell migration. *Bioessays* **15,** 221–230.

Buisson, A. C., Zahm, J. M., Polette, M., Pierrot, D., Bellon, G., Puchelle, E., Birembaut, P., and Tournier, J. M. (1996). Gelatinase B is involved in the in vitro wound repair of human respiratory epithelium. *J. Cell Physiol.* **166,** 413–426.

Bullard, K. M., Cass, D. L., Banda, M. J., and Adzick, N. S. (1997). Transforming growth factor beta-1 decreases interstitial collagenase in healing human fetal skin. *J. Pediatr. Surg.* **32,** 1023–1027.

Carinato, M. E., Walter, B. E., and Henry, J. J. (2000). *Xenopus laevis* gelatinase B (Xmmp-9): Development, regeneration, and wound healing. *Dev. Dyn.* **217,** 377–387.

Choi, B. M., Kwak, H. J., Jun, C. D., Park, S. D., Kim, K. Y., Kim, H. R, and Chung, H. T. (1996). Control of scarring in adult wounds using antisense transforming growth factor beta-1 oligodeoxynucleotides. *Immunol. Cell Biol.* **74,** 144–150.

Christensen, R. N., and Tassava, R. A. (2000). Apical epithelial cap morphology and fibronectin gene expression in regenerating *Axolotl* limbs. *Dev. Dyn.* **217,** 216–224.

Cunha, G. R. (1994). Role of mesenchymal–epithelial interactions in normal and abnormal development of the mammary gland and prostate. *Cancer* **74,** 1030–1044.

Damjanovsky, S., Ishizuya-Oka, A., and Shi, Y. B. (1999). Spatial and temporal regulation of collagenases-3, -4 and stromelysin-3 implicates distinct functions in apoptosis and tissue remodeling during frog metamorphosis. *Cell Res.* **9,** 91–105.

Damjanovsky, S., Puzianowska-Kuznicka, M., Ishizuya-Oka, A., and Shi, Y. B. (2000). Differential regulation of three thyroid hormone-responsive matrix metalloproteinases genes implicates distinct functions during frog embryogenesis. *FASEB J.* **14,** 503–510.

Garat, C. F., Heradmand, K., Albertine, K. H., Folkesson, H. G., and Matthay, M. A. (1996). Soluble and insoluble fibronectin increases alveolar epithelial wound healing in vitro. *Am. J. Physiol.* **271,** L844–L853.

García-Arrarás, J. E., Estrada, L., Santiago, R., Torres, I., and Torres-Avilán, I. (1998). Cellular mechanisms in the regeneration of the intestine of the sea cucumber, *Holothuria glaberrima selenka. J. Exp. Zool.* **281,** 288–304.

García-Arrarás, J. E., Diaz-Miranda, L., Torres, I. I., Files, S., Jimenez, L. B., Rivera-Bermudez, K., Arroyo, E. J., and Cruz, W. (1999). Regeneration of the enteric nervous system in the sea cucumber, *Holothuria glaberrima. J. Comp. Neurol.* **406,** 461–475.

Gassner, K. M., and Tassava, R. A. (1997). Abnormal limb regeneration in the short-toes mutant of the axolotl, *Ambystoma mexicanum*: Studies of age, level of amputation, and extracellular matrix. *J. Exp. Zool.* **279,** 571–578.

Ghiglione, C., Lhomond, G., LePage, T., and Gache, C. (1994). Structure of the sea urchin hatching enzyme gene. *Eur. J. Biochem.* **219,** 845–854.

Goke, M., Zuk, A., and Podolsky, D. K. (1996). Regulation and function of extracellular matrix intestinal epithelial restitution in vitro. *Am. J. Physiol.* **271,** G729–G740.

Grant, G. A., Eizen, A. Z., Marmer, B. L., Roswit, W. T., and Goldbegr, G. I. (1987). The activation of human skin fibroblast procollagenases: Sequence identification of the major conversion products. *J. Biol. Chem.* **262,** 5886–5889.

Haralson, M. A., and Hassell, J. R. (1995). "Extracellular Matrix: A Practical Approach." Oxford University Press, New York.

Haruyama, T., Ajioko, I., Akaike, T., and Watanabe, Y. (2000). Regulation and significance of hepatocyte-derived matrix metalloproteinases in liver remodeling. *Biochem. Biophys. Res. Commun.* **272,** 681–686.

Haffen, K., Lacroix, B., Kedinger, M., and Simon-Assmann, P. M. (1983). Inductive properties of fibroblastic cell cultures derived from rat intestinal mucosa on epithelial differentiation. *Differentiation* **23,** 226–233.

Harlow, E., and Lane D. (1988). "Antibodies: A Laboratory Manual," pp. 196–219. Cold Spring Harbor Laboratory Press, Cold Spring Harbor, NY.

Hyman, L. (1955). "The Invertebrates: Echinodermata." McGraw-Hill Book Co., New York.

Ingersoll, E. P., and Wilt, F. H. (1998). Matrix metalloproteinases inhibitors disrupt spicule formation by primary mesenchyme cells in the sea urchin embryo. *Dev. Biol.* **196,** 95–106.

Kedinger, M., Simon, P. M., Grenier, J. F., and Haffen, K. (1981). Role of epithelial-mesenchymal interactions in the ontogenesis of intestinal brush border enzymes. *Dev. Biol.* **86,** 339–347.

Kherif, S., Lafuma, C., Dehaupas, M., Lachkar, S., Fournier, J. G., Verdiere-Sahuque, M., Fardeau, M., and Alameddine, H. S. (1999). Expression of matrix metalloproteinases 2 and 9 in regenerating skeletal muscle: A study in experimentally injured and mdx muscles. *Dev. Biol.* **205,** 158–170.

Kim, T. H., Mars, W. M., Stolz, D. B., Petrsen, B. E., and Michalopoulos, G. K. (1997). Extracellular matrix remodeling at the early stages of liver regeneration in the rat. *Hepatology* **26,** 896–904.

Knittel, T., Mehde, M., Grundmann, A., Saile, B., Scharf, J. G., and Ramadori, G. (2000). Expression of matrix metalloproteinases and their inhibitors during hepatic tissue repair in the rat. *Histochem. Cell Biol.* **113,** 443–453.

Kreis, T., and Vale, R. (1994). "Guidebook to the Extracellular Matrix and Adhesion Proteins." Oxford University Press, New York.

Kurisu, K., Ohsaki, Y., Nagata, K., Kukita, T., Yoshikawa, H., and Inai, T. (1987). Immunoelectron microscopic localization of fibronectin in the smooth muscle layer of mouse small intestine. *J. Histochem. Cytochem.* **35,** 411–417.

Leontovich, A. A., Zhang, J., Shimokawa, K., Nagase, H., and Sarras, M. P. (2000). A novel hydra metalloproteinase (HMMP) functions in extracellular matrix degradation, morphogenesis and the maintenance of differentiated cells in the foot prcess. *Development* **127,** 907–920.

Lhomond, G., Ghiglione, C., LePage, T., and Gache, C. (1996). Structure of the gene encoding the sea urchin blastula protease 10 (BP10), a member of the astacin family of Zn++-metalloprotease. *Eur. J. Biochem.* **238,** 744–751.

Lin, R. Y., Sullivan, K. M., Argenta, P. A., Meuli, M., Lorenz, H. P., and Adzick, N. S. (1995). Exogenous transforming growth factor-beta amplifies its own expression and induces scar formation in a model of human fetal skin repair. *Ann. Surg.* **222,** 146–154.

Lovvorn, H. N., Cheung, D. T., Nimni, M. E., Perelman, N., Estes, J. M., and Adzick, N. S. (1999). Relative distribution and crosslinking of collagen distinguish fetal from adult sheep wound repair. *J. Pediatr. Surg.* **34,** 218–223.

Martin, P. (1997). Wound healing: Aiming for perfect skin regeneration. *Science* **276,** 75–87.

Massova, I., Kotra, L. P, Fridman, R., and Mobashery, S. (1998). Matrix metalloproteinases: Structures, evolution, and diversification. *FASEB J.* **12,** 1075–1095.

Mast, B. A., Albanese, C. T., and Kapadia, S. (1998). Tissue repair in the fetal intestinal tract occurs with adhesions, fibrosis, and neovascularization. *Ann. Plast. Surg.* **41,** 140–147.

Matrisan, L. M. (1990). Metalloproteinases and their inhibitors matrix remodeling. *Trends Genet.* **6,** 121–125.

Matrisan, L. M. (1992). The matrix degrading metalloproteinases. *Bioessays* **14,** 455–463.

Mayne, J., and Robinson, J. J. (1996). Purification and metal ion requirements of a candidate matrix metalloproteinase: A 41 kDa gelatinase activity in the sea urchin embryo. *Biochem. Cell Biol.* **74,** 211–218.

Meuli, M., Lorenz, H. P., Hedrick, M. H., Sullivan, K. M., Harrison, M. R., and Adzick, N. S. (1995). Scar formation in the fetal alimentary tract. *J. Pediatr. Surg.* **30,** 392–395.

Miyazaki, K., Uchiyama, K., Yutaka, I., and Katsutoshi, Y. (1996). Cloning and characterization of cDNAs for matrix metalloproteinases of regenerating newt limbs. *Proc. Natl. Acad. Sci. USA* **93,** 6819–6824.

Moore, W. M., and Spilburg, C. A. (1986a). Peptide hydroxamic acids inhibit skin collagenase. *Biochem. Biophys. Res. Commun.* **136,** 390–395.

Moore, W. M., and Spilburg, C. A. (1986b). Purification of human collagenases with hydroxamic acid affinity column. *Biochemistry* **25,** 5189–5195.

Mosher, C. (1956). Observation on evisceration and visceral regeneration in the sea cucumber, *Actinopyga agassizi* Selenka. *Zoologica* NY **41,** 17–26.

Nace, J. D., and Tassava, R. A. (1995). Examination of fibronectin distribution and its sources in the regenerating newt limb by immunocytochemistry and in situ hybridization. *Dev. Dyn.* **202,** 153–164.

Nagase, H., and Woessner, J. F. (1999). Matrix metalloproteinases. *J. Biol. Chem.* **274,** 21491–21494.

Odake, S., Morita, Y., Morikawa, T., Yoshida, N., Hori, H., and Nagai, Y. (1994). Inhibition of matrix metalloproteinases by peptidyl hydroxamic acids. *Biochem. Biophys. Res. Commun.* **199,** 1442–1446.

Park, I. S., and Kim, W. S. (1999). Modulation of gelatinase activity correlates with the dedifferentiation profile of regenerating salamander limbs. *Mol. Cell* **9,** 119–126.

Patterton, D., Hayes, W. P., and Shi, Y. (1995). Transcriptional activation of the metalloproteinase gene stromelysin-3 coincides with thyroid hormone-induced cell death during frog metamorphosis. *Dev. Biol.* **167,** 252–262.

Pohle, T., Drees, M., Gillessen, A., Shanin, M., Voss, B., and Domshke W. (1997). Simultaneous restitution of matrix and cells in gastric ulcer: Use of a combined in-situ hybridization and immunohistochemistry technique applicable to paraffin embeded tissue. *Cell Tissue Res.* **287,** 601–610.

Quigley, J. P., Braithwait, R. S., and Amstrong, P. B. (1993). Matrix metalloproteases of the developing sea urchin embryo. *Differentiation* **54,** 19–23.

Ramachandran, R. K., Seid, C. A., and Tomlinson, C. R. (1993). PDGF-BB and TGF-αrescue gastrulation, spiculogenesis, and LpS1 expression in collagen-disrupted embryos of the sea urchin genus Lytechinus. *Mech. Dev.* **44,** 33–40.

Robinson, J. J. (1997). Characterization of a metalloproteinase: A late specific gelatinase activity in the sea urchin embryo. *J. Cell Biochem.* **66,** 337–345.

Roe, J. L., Park, H. R., and Lennarz, W. J. (1989). Inhibitors of metalloproteases block spiculogenesis in sea urchin primary mesechyme cells. *Exp. Cell Res.* **181,** 542–550.

Rooney, P., and Kumar, S. (1993). Inverse relationship between hyaluronan and collagens in development and angiogenesis. *Differentiation* **54,** 1–9.

Sanberg, M., Tamminem, M., Hirvonem, H., and Pihlajaniemi, T. (1989). Expression of mRNAs coding for the α-chain of type XIII collagen in human fetal tissues: Comparison with expression for collagen type I, II, and III. *J. Cell Biol.* **109,** 1371–1379.

Schedin, P., Strange, R., Mitrenga, T., Wolfe, P., and Kaeck, M. (2000). Fibronectin fragments induce MMP activity in mouse mammary epithelial cells: Evidence for a role in mammary tissue remodeling. *J. Cell Sci.* **113,** 795–806.

Seifert, W. F., Wobbes, T., and Hendriks, T. (1996). Divergent patterns of matrix metalloproteinases activiy during wound healing in ileum and colon of rats. *Gut* **39,** 114–119.

Seifert, W. F., Wobbes, T., and Hendriks, T. (1997). Intra-operative irradiation prolongs the matrix metalloproteinase activity in large bowel anastomoses of the rat. *Radiat. Res.* **147,** 354–361.

Sheppard, A. M., Hamilton, S. K., and Pearlman, A. L. (1991). Changes in the distribution of extracellular matrix components accompany early morphogenetic events of mammalian cortical development. *J. Neurosci.* **11,** 3928–3942.

Sheppard, A. M., Brunstrom, J. E., Thornton, T. N., Gerfen, R. W., Broekelmann, T. J., McDonald, J. A., and Pearlman, A. L. (1995). Neuronal production of fibronectin in the cerebral cortex during migration and layer formation is unique to specific cortical domains. *Dev. Biol.* **172,** 504–518.

Simo, P., Simon-Assmann, P., Bouziges, F., Leberquier, C., Kedinger M., Ekblom, P., and Sorokin, L. (1991). Changes in the expression of laminin during intestinal development. *Development* **112,** 477–487.

Simon-Assmann, P., Kedinger, M., De Arcangelis, A., Rosseau, V., and Simo, P. (1995). Extracellular matrix components in intestinal development. *Experientia* **51,** 883–900.

Simon-Assmann, P., Kedinger, M., and Haffen, K. (1986). Immunocytochemical localization of extracellular matrix proteins in relation to rat intestinal morphogenesis. *Differentiation* **32,** 59–66.

Simoneau, A., Herring-Gillam, F. E., Vachon, P. H., Perreault, N., Basora N., Bouatrouss, Y., Pageot, L. P., Zhou, J., and Bealieu, J. F. (1998). Identification, distribution, and tissular origin of the alpha5(IV) and alpha6(IV) collagen chains in the developing human intestine. *Dev. Dyn.* **212,** 437–447.

Spiegel, E., Burger, M., and Spiegel, M. (1983). Fibronectin and laminin in the extracellular matrix and basement membrane of sea urchin embryos. *Exp. Cell Res.* **144,** 47–55.

Talhouk, R. S., Chin, J. R., Unemori, E. N., Werb, Z., and Bissell, M. J. (1991). Proteinases of the mammary gland: Developmental regulation *in vivo* and vectorial secretion in culture. *Development* **112,** 439–449.

Taniyama, Y., Morishita, R., Nakagami, H., Moriguchi, A., Sakonjo, H., Shokei-Kim, Matsumoto, K., Nakamura, T., Higaki, J., and Ogihara, T. (2000). Potential contribution of a novel antifibrotic factor, hepatocyte growth factor, to prevention of myocardial fibrosis by angiotensin II blockade in cardiomyophatic hamster. *Circulation* **102,** 246–252.

Tanney, D. C., Feng, L., Pollock, A. S., and Lovett, D. H. (1998). Regulated expression of matrix metalloproteinases and TIMP in nephrogenesis. *Dev. Dyn.* **213,** 121–129.

Thesleff, I., Vaahtokari, A., and Partanen, A. M. (1995). Regulation of organogenesis. Common molecular machanism regulating the development of teeth and other organs. *Int. J. Dev. Biol.* **39,** 35–50.

Uria, J. A., and Werb, Z. (1998). Matrix metalloproteinases and their expression in mamary gland. *Cell Res.* **8,** 187–194.

Vafa, O., Goetzl, L., Poccia, D., and Nishioka, D. (1996). Localization and characterization of blastocoelic extracellular matrix antigens in early sea urchin embryos and evidence for their proteolytic modification during gastrulation. *Differentiation* **60,** 129–138.

Vafa, O., and Nishioka, D. (1995). Developmentally regulated protease expression during sea urchin embryogenesis. *Mol. Reprod. Dev.* **40,** 36–47.

VandenSpiegel, D., Jangaoux, M., and Flammang, P. (2000). Maintaining the line of defense: Regeneration of cuvierian tubules in the sea cucumber *Holothuria forskali* (Echinodermata, *Holothurioidea*.) *Biol. Bull.* **198,** 34–49.

Wallner, E. I., Yang, Q., Peterson, D. R., Wada, J., and Kanwar, Y. S. (1998). Relevance of extracellular matrix, its receptors, and cell adhesion molecules in mammalian nephrogenesis. *Am. J. Physiol.* **275,** F467–F477.

Wardle, F. C., Angerer, L. M., Angerer, R. C., and Dale, R. (1999). Regulation of BMP1/TLD-related metalloprotease, SpAN. *Dev. Biol.* **206,** 63–72.

Wessel, G. M., and McClay, D. R. (1987). Gastrulation in the sea urchin embryo requires the deposition of crosslinked collagen within the extracellular matrix. *Dev. Biol.* **121,** 149–165.

Wessel, G. M., Marchase, R. B., and McClay, D. R (1984). Ontogeny of the basal lamina in the sea urchin embryo. *Dev. Biol.* **103**, 235–245.

Witty, J. P., Wright, J. H., and Matrisian, L. M. (1995). Matrix metalloproteinases are expressed during ductal and alveolar mammary morphogenesis, and misregulation of stromelysin-1 in trensgenic mice induces unscheluded alveolar development. *Mol. Biol. Cell* **6,** 1287–1303.

Yan, L., Fei, K., Shang, J., Dexter, S., and Sarras, M. P. (2000a). Identification and characterization of hydra metalloproteinases 2 (HMP2): A meprin like astacin metalloproteinase that function in foot morphogenesis. *Development* **127,** 129–141.

Yan, L., Leontovich, A., Fei, K., and Sarras, M. P. (2000b). Hydra metalloproteinase 1: A secreted astacin metalloproteinase whose apical axis expression is differentially regulated during head regeneration. *Dev. Biol.* **219,** 115–128.

Yang, E. V, and Bryant, S. V. (1994). Developmental regulation of a matrix metalloproteinase during regeneration of axolotl appendages. *Dev. Biol.* **166,** 696–703.